

Influence of ZnS Sputtering Power on Film Adhesion and $\text{Cu}_2\text{ZnSnS}_4$ Solar Cells

Wang Lu¹, Guo Jie^{1*}, Hao Ruiting^{2*}, A. Aierken², Sun Lichun¹, Qiong Li², Liu Bin¹, Gu Kang², Sun Shuaihui¹

¹ Yunnan Key Laboratory of Optoelectronic Information Technology, Yunnan Normal University, Kunming, Yunnan, 650500, People's Republic of China

² Key Laboratory of Renewable Energy Advanced Materials and Manufacturing Technology Ministry of Education, Yunnan Normal University, Kunming, Yunnan, 650500, People's Republic of China

The stacking precursors Mo/ZnS/SnS/Cu were sputtered on soda-lime glass (SLG) substrates using different sputtering power of ZnS changing from 50 W to 140 W. $\text{Cu}_2\text{ZnSnS}_4$ (CZTS) thin films were obtained by annealing the precursors. The effects of ZnS sputtering powers on the morphology, microstructure and adhesion in ZnS and followed CZTS thin films were investigated. ZnS thin films with different power were hexagonal wurtzite with (008) preferred orientation. The compressive stress in ZnS thin film increased by an order of magnitude with sputtering power from 50 W to 140 W. When sputtering power of ZnS was lower than 80 W or higher than 110 W, the crack and even falling off phenomenon were observed in the annealed CZTS thin films. From 80 W to 110 W, the surface of CZTS thin film was even but more holes and secondary phases appeared at higher power of 110 W. The CZTS solar cell was fabricated with ZnS thin films sputtered at 80 W, which showed the open circuit voltage of 572 mV, the short circuit current density of 14.23 mA/cm² and the conversion efficiency of 3.34 %.

Keywords: $\text{Cu}_2\text{ZnSnS}_4$, ZnS, stress, films adhesion

INTRODUCTION

$\text{Cu}_2\text{ZnSnS}_4$ (CZTS) is a direct bandgap semiconductor material, with band gap of 1.4~1.5 eV. It has similar photovoltaic performance to $\text{CuIn}_x\text{Ga}(1-x)\text{Se}_2$, making it an ideal absorber layer for thin film solar cells. Besides, CZTS solar cells attract the attention of researchers all over the world because of earth-abundant elements and non-toxic, [1-6]. In 2013, IBM Corporation, Solar Frontier and Tokyo Chemical Industry Co., Ltd. jointly developed CZTSSe thin-film solar cell with photoelectric conversion efficiency of 12.6%, which is the highest in copper-based solar cell [7], but it still far from the theoretical maximum efficiency of 31% [8],[9]. The magnetron sputtering has the advantages of flexible target selection and easy control of deposition parameters. Araki et al. [10] reported the effect of six different stacking orders on the properties of CZTS films, and the Mo/Zn/Cu/Sn structure was optimized with an efficiency of 1.79 %. Katagiri et al. [11] prepared CZTS thin films by co-sputtering Cu/ZnS/SnS targets, studying the effect of sulfurization on phase formation. Katagiri et al. [12] also reported that the annealing caused the loss of Zn and Sn, resulting in

the conversion efficiency decreasing. The Zn and Sn elemental targets are replaced by the binary sulfide targets ZnS and SnS, which can further promote grain growth and reduce formation of secondary phases and the holes on the surface of the CZTS film [13][14]. Shin et al. studied three different structures of CZTS precursors and found that Mo/ZnS/SnS₂/Cu sequence can obtain better phase purity [15]. However, the residual stress of films could be affected by the growth process like the temperature or the power [16]. Li et al. found that the films had crack and peel off after annealing in magnetron-sputtered CZTSSe. Since the thermal expansion coefficient of Cu and its sulfide is higher than that of ZnS and SnS, a large stress occurs. Placing Cu on the top layer, as SLG/Mo/ZnS/SnS/Cu, will reduce the possibility of film cracking and shedding [17]. On the other hand, in process of sputtering, the internal stress of ZnS thin film will not only lead to red shift of absorption edge and narrow band gap [18-20], [23], but also cause films to crack or even fall off after annealing. In the growth conditions of ZnS thin films, sputtering power has a great influence on structure, grain growth and surface roughness, it also one of the important factors affecting film stress and

To whom all correspondence should be sent:

E-mail: ynnugj@sohu.com

adhesion [13],[18]. The quality of ZnS thin film as bottom layer has crucial influence on the crystal quality, photoelectric performance and internal stress of CZTS thin film. In this paper, the CZTS precursor was prepared by sputtering Mo/ZnS/SnS/Cu. ZnS thin films were sputtered with different powers. The influence of sputtering power on the structure, morphology, adhesion and photovoltaic performance of CZTS films and solar cells were studied.

EXPERIMENTAL

CZTS thin film precursors were deposited at room temperature on 20mm × 20mm soda lime glasses by magnetron sputtering Mo, ZnS, SnS, and Cu target in sequence. The background vacuum was 10⁻⁵ Pa and Ar pressure was 0.3 Pa. The Mo bottom electrodes about 1.2 μm thickness were firstly sputtered under 100 W power. The sputtering parameters were shown in Tab.1. The sputtering power of ZnS is 50 W, 80 W, 110 W, and 140 W, with the composition of precursors was adjusted to Cu/(Zn+Sn) ≈ 0.8 and Zn/Sn ≈ 1.2. The four samples at different ZnS power were marked as A1, A2, A3 and A4 respectively. After characterizing the crystal structure of ZnS, SnS with 50 W power and Cu with 100 W power were sputtered on ZnS. The precursors were placed in a graphite boat and annealed in the furnace filling with high-purity nitrogen gas to remove air. The heating temperature was 260°C for 30 minutes then cooling in nature. Then, the temperature was raised to 580 °C for 30 min in sulfur powder and a CZTS film was obtained. The surface and cross-section morphology, crystal structure of ZnS and CZTS thin films were characterized by field emission scanning electron microscopy (SEM: FEI Nova Nano450) and X-ray diffraction (XRD: Rigaku Ultima IV). Hereafter, the 50 nm thick CdS as buffer layer was deposited on the CZTS film by chemical bath method (CBD). The window layer i-ZnO (50 nm) and ZnO:Al (200 nm) were prepared by RF sputtering. The current density-voltage (J-V) characteristics of the CZTS solar cells were measured by a solar simulator under the standard AM1.5 spectrum using a Keithley 2420 source meter unit. The whole sample of 20mm×20mm area was illuminated with the intensity of 100 mW/cm². The light intensity of the solar simulator was calibrated with a standard monocrystalline Si reference solar cell. Finally, the top grids electrodes of Au with 150nm thickness were fabricated by thermal evaporation.

Table 1. Sputtering parameters for ZnS

Target	Sample	Sputtering power		Film thickness
		[W]		[nm]
ZnS	A1	50		270.4
	A2	80		221.0
	A3	110		196.9
	A4	140		152.6

RESULTS AND DISCUSSION

Morphology and structure

As shown in Fig.1, SEM images of four samples have uniform surface, clear grain boundary and no cracks. With increase of sputtering power, the grain size of ZnS increased gradually due to the increasing of atoms energy and surface migration. The atoms are likely to aggregate resulting in an increase in grain size [21].

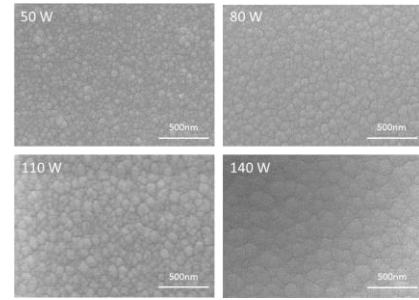


Fig.1. SEM images of ZnS films at different sputtering power

Fig.2 showed XRD patterns of ZnS thin films at different sputtering power. Three peaks at $2\theta=28.5^\circ$, 47.5° , 56.3° , which correspond to (008), (110) and (118) diffraction planes in the hexagonal structure.

The microstructure parameters of ZnS films at different sputtering power was shown in Tab.2. As sputtering power increased from 50W to 140W, the (008) diffraction peak intensity increased by six times with the full width at half maximum (FWHM) decreasing. In addition, a smaller angle shift of (008) peak position indicated the lattice constant became larger.

The lattice difference will result in the residual stress in the film. The calculation of the film stress is based on the biaxial strain model [22]. The strain along the c-axis ϵ_{zz} can be estimated by the relation:

$$\epsilon_{zz} = \frac{C_{film} - C_{bulk}}{C_{bulk}} \quad (1)$$

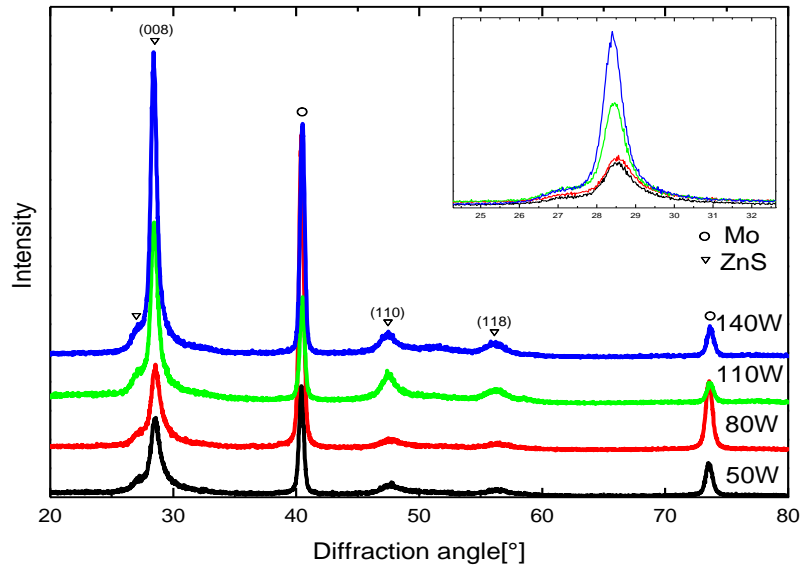


Fig.2. XRD patterns of ZnS films at different sputtering power

Table 2. Microstructure parameters of ZnS films at different sputtering power

Sputtering power [W]	2θ [°]	Intensity	FWHM	Lattice a_o [Å]	Residual stresses [GPa]
bulk	28.602	—	—	3.1183	0
50	28.579	3908.33	0.666	3.1208	-0.1866
80	28.559	7508.33	0.633	3.1229	-0.3430
110	28.460	15833.3	0.574	3.1336	-1.1422
140	28.400	26575.0	0.525	3.1400	-1.6201

Being c_{bulk} the strain-free lattice constant of bulk ZnS (3.1183 Å) and c_{film} the lattice constant of ZnS films measured by XRD. Further, the biaxial film stress σ is related to the measured c-axis strain by the relation:

$$\sigma_{film} = \frac{2c_{13}^2 - c_{33}(c_{11} + c_{12})}{2c_{13}} \cdot \epsilon_{zz} \quad (2)$$

For the elastic constants c_{ij} , the data of single crystalline ZnS have been used: $c_{11}=208.8$, $c_{33}=213.8$, $c_{12}=119.7$, $c_{13}=104.2$ GPa. [21] The residual stresses of all ZnS thin film showed the compressive stress, and increased by an order of magnitude as the power increases from 50W to 140W.

Morphology and structure of CZTS thin Films with different ZnS power

CZTS thin films images with different

ZnS sputtering power before and after annealing were shown in Fig.3. The four precursors before annealing has smooth and dense surface as shown in Fig.3a. During annealing treatment, sample A1 and A4 had obvious cracking and peeling. The poor crystal quality of ZnS at low power resulted in the poor adhesion in A1. The peeling of A4 may be due to the thermal expansion coefficient differency between the substrates and Cu, SnS layers. The interface stress was caused by the structural mismatching of small grain of A1 and large grain of A4. These stresses lead films to poor adhesion, resulting in cracking and shedding [24, 25]. On the contrary, sample A2 and A3 did not crack or fall off, which indicated that sputtering power of ZnS was between 80W and 110W can bring lower stress and better crystal quality of ZnS and CZTS films.

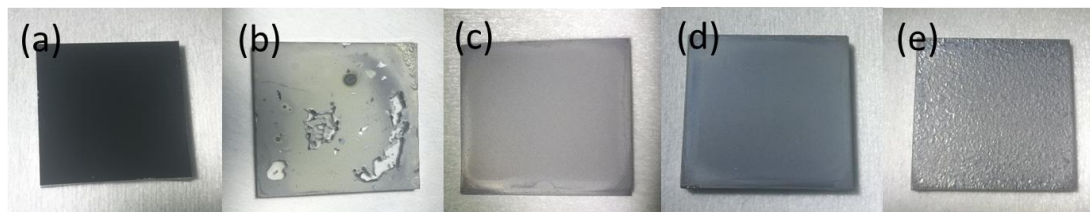


Fig.3 CZTS films images before annealing (a) and after annealing at different ZnS power 50 W (b), 80 W (c), 110 W (d) and 140 W (e)

The surface and section morphology of A2 and A3 samples were analysed by SEM as shown in Fig.4. The surface grains of CZTS film in A2 are larger than that in A3. There were obvious pores and cracks on the surface of A3 (Fig.4c). Fig.4b showed more than $2\mu\text{m}$ grain and dense morphology in

A2. The A3 was non-uniformity with many small grains and holes at the bottom as shown in Fig.4d. The holes will cause the traps and the recombination centers at the CZTS/Mo interface, reducing the photoelectric conversion efficiency of CZTS solar cells [26].

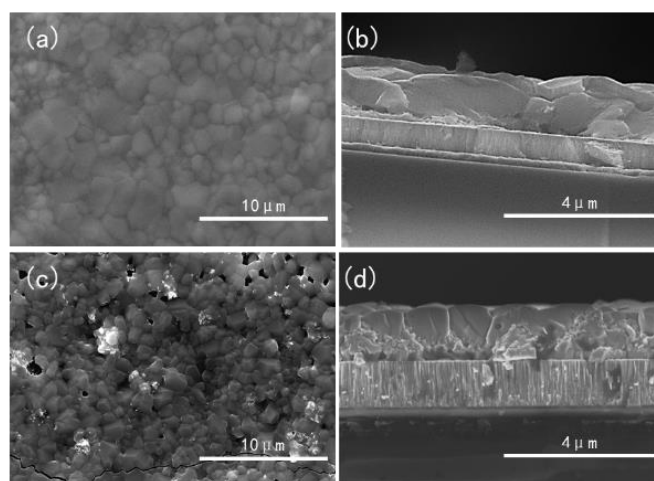


Fig.4. SEM images of surface and cross-section in sample A2 (a, b) and A3 (c, d)

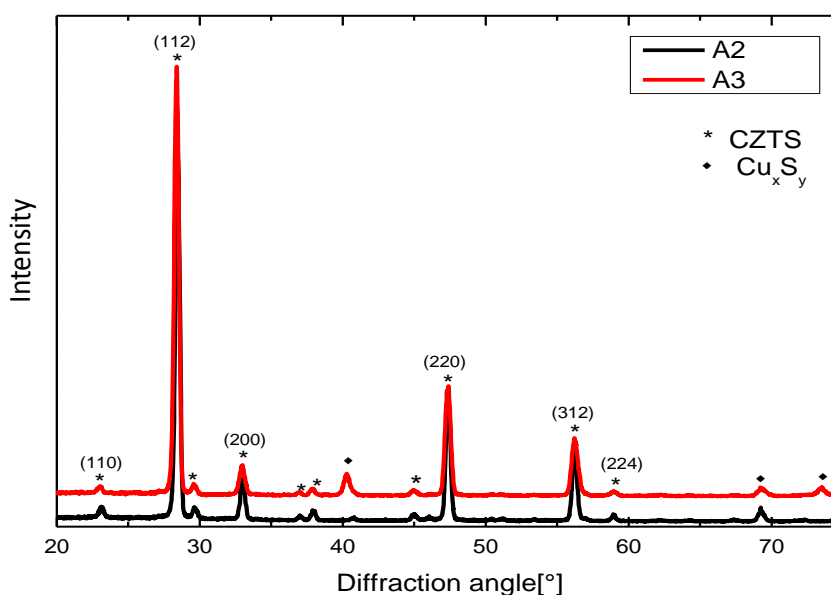


Fig.5. XRD patterns of sample A2 and A3

The reaction mechanism of CZTS films has been studied deeply [27, 28]. Due to the strong migration ability of Cu, it will firstly react with SnS to form a mesophase Cu₂SnS₃, then react with Zn to form CZTS. Fig.5 was XRD pattern of the sample A2, A3 after annealing. Three main diffraction peaks at $2\theta = 28.53^\circ, 47.33^\circ, 56.18^\circ$ corresponded to the (112), (220), (312) crystal planes, correlating well with ICDD value of kesterite CZTS (ICDD No: 00-026-0575). Compared with A2, A3 had a Cu_xS_y phase ($x=1.9, 3.1; y=1.5, 1.6$), Cu₂SnS₃, and SnS phases at $2\theta = 40.4^\circ, 69.3^\circ$ and 73.6° . The formation of these secondary phases may be due to the higher sputtering power to obtain a dense ZnS film, which cannot be fully combined with the Cu₂SnS₃ phase to form Cu₂ZnSnS₄.

Electrical characteristics of CZTS solar cells

The *J-V* curve of CZTS solar cells fabricated by A2 and A3 thin films were shown in Fig.6. CZTS solar cell fabricated by A2 had better short-circuit current of 14.23 mA/cm² and fill factor of 0.41, thus having relatively higher photoelectric conversion efficiency of 3.3%. The open voltage of the two samples was close. The short current of sample A3 was inferior due to the more traps which enhanced the photogenerated carrier nonirradiation recombination at the CZTS/Mo interface as shown in the SEM images in Fig.4. Further, the secondary phases with insufficient react also led to the increase of series resistance [29]. Experiments showed that under fixed conditions, when sputtering power of ZnS was about 80 W, the CZTS solar cell obtained better photoelectric performance.

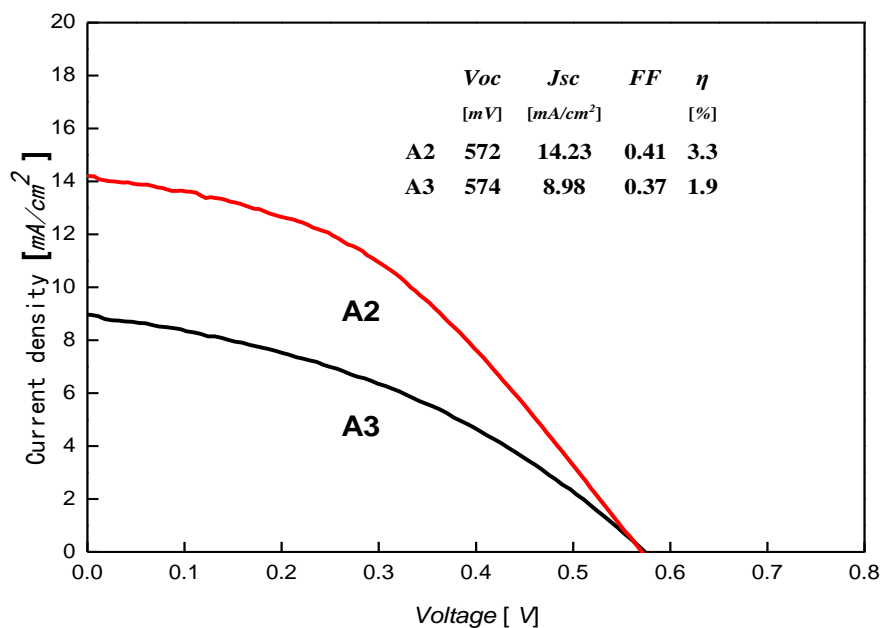


Fig.6. *J-V* curve and the photoelectrical performance for A2 and A3 solar cells

CONCLUSION

CZTS solar cells were prepared by magnetron sputtering with stacking sequence SLG/Mo/ZnS/SnS/Cu. The adhesion was a crucial influence factor on the quality of the thin films. In this paper, the adhesion of CZTS thin film was optimized by adjusting the sputtering power of ZnS, which is helpful to increase the

yield rate for the low-cost solar cell fabrication and other functional material including ZnS thin films. The film morphology and crystal structure were studied under the sputtering power of ZnS from 50 W to 140 W. The results showed that residual stress would remain in the film which would crack or even fall off when the power lower than 80 W and higher than 110 W. The photoelectric conversion efficiency of CZTS solar cells under the optimal ZnS

power was 3.3%. However, the effects of other factors such as the temperature on the adhesion still need to be explored, and the efficiency of CZTS solar cell will be anticipated to improve.

ACKNOWLEDGEMENTS

This study was supported by the National Natural Science Foundation of China (No. 61774130, 61705192, 61534008).

REFERENCES

- [1] A Walsh, S Chen, S Wei, Kesterite Thin-Film Solar Cells: Advances in Materials Modelling of Cu₂ZnSnS₄. *Advanced Energy Materials* **2**, 400-409 (2012).
- [2] D B Mitzi, O Gunawan, T K Todorov, The path towards a high-performance solution-processed kesterite solar cell. *Solar Energy Materials and Solar Cells* **95**, 1421-1436 (2011).
- [3] A Polizzotti, I L Repins, R Noufi, et al. The state and future prospects of kesterite photovoltaics. *Energy & Environmental Science* **6**, 3171-3182 (2013).
- [4] T K Todorov, J Tang, S Bag, et al. Beyond 11% efficiency: characteristics of state-of-the-art Cu₂ZnSn(SSe)₄ solar cells. *Advanced Energy Materials* **3**, 34-38 (2013).
- [5] G. Raikova, P. Carpanese, Z. Stoyanov; D. et al. Inductance correction in impedance studies of solid oxide fuel cells. *Bulgarian chemical communications* **41**, 199-206 (2009).
- [6] G. Krishnamurthy, M. Sona Bai, Oxidation of lindane in contaminated water under solar irradiation in the presence of photocatalyst and oxidizing agents. *Bulgarian chemical communications* **42**, 161-166 (2010).
- [7] W. Wang, M. T. Winkler, O. Gunawan, Device Characteristics of CZTSSe Thin Film Solar Cells with 12.6% Efficiency. *Adv. Energy Mater.* **4**, 1029-1036 (2014).
- [8] W. Shockley, H. Queisser, Detailed Balance Limit of Efficiency of pn Junction Solar Cells, *J. Appl. Phys.* **32**, 510-519 (1961).
- [9] C. Henry, Limiting efficiencies of ideal single and multiple energy gap terrestrial solar cells, *J. Appl. Phys.* **51**, 4494-4500 (1980)
- [10] H. Araki, et al., Preparation of Cu₂ZnSnS₄ thin films by sulfurization of stacked metallic layers, *Thin Solid Films* **517**, 1457-1460 (2008).
- [11] H. Katagiri, K. Jimbo, M. Tahara, The influence of the composition ratio on CZTS-based thin film solar cells, *Proc. of Mater. Res. Soc. Symp.* **113**, 1165-M04 (2009).
- [12] H Katagiri, K Saitoh, Development of thin film solar cell based on Cu₂ZnSnS₄ thin films. *Solar Energy Materials and Solar Cells* **65**, 141-148 (2001).
- [13] D H Son, D H Kim, S N Park, Growth and Device Characteristics of CZTSSe Thin-Film Solar Cells with 8.03% Efficiency. *Chem. of Mater.* **2**, 5180-5188 (2015).
- [14] J. Li, Y. Zhang, H. Wang, On the growth process of Cu₂ZnSn(SSe)₄ absorber layer by selenizing Cu₂ZnSn(SSe)₄ precursors and its photovoltaic performance, *Sol. Energy Mater. Sol. Cells* **132**, 363-371 (2015).
- [15] Shin S W, Pawar S M, Park C Y, Studies on Cu₂ZnSnS₄ (CZTS) absorber layer using different stacking orders in precursor thin films. *Solar Energy Materials and Solar Cells* **95**, 3202-3206 (2011).
- [16] S Y Shao, Z X Fan, J D Shao, Study of Residual Stress in ZrO₂ Thin Films, *Acta Opt. Sin.* **24**, 437-441 (2004)
- [17] Li J J, Fabrication and research of CZTSSe thin film solar cells by magnetron sputtering and post-selenization process, Ph.D's Thesis, Tianjin, Nankai University, 2016
- [18] A. Le Donne, D. R.A Cavalcoli, M Mereu, Study of the physical properties of ZnS thin films deposited by RF sputtering. *Mater. Sci. in Semi. Processing* **71**, 128-130 (2017).
- [19] G Laukaitis, S Lindroos, S Tamulevicius, Stress and morphological development of CdS and ZnS thin films during the SILAR growth on GaAs, *Appl. Surf. Sci.* **185**, 134-139 (2001).
- [20] S Rodrigues, A G Rolo, A Khodorov, Determination of residual stress in PZT films produced by laser ablation with X-ray diffraction and Raman spectroscopy, *J. Euro. Ceram. Soc.* **30**, 521-525, (2010).
- [21] P F Gui, Z R Zheng, Y J Zhao, Study on the mechanism and measurement of stress of TiO₂ and SiO₂ thin-films, *Acta Phys. Sin.* **55**, 6459 (2006)
- [22] A. Segmuller, M. Murakami, In Analytical Techniques for Thin Films, Springer, 1988.
- [23] E. Mollwo, In Landoldt-Börnstein. Zahlenwerte und Funktionen aus

- Naturwiss. u. Technik. Neue Serie, Springer, 1982.
- [24] J Xie, B Li, Y J Li, Study on ZnS thin films prepared by RF magnetron sputtering technique, *Acta. Phys. Sin.* **59**, 5749-5754 (2010).
- [25] X P Song, X Yang, Study on preparation and properties of ZnS thin films, *Journal of Functional Materials* **11**, 1734-1736 (2006).
- [26] C. Hong, S. Shin, K. Gurav, Comparative study on the annealing types on the properties of $\text{Cu}_2\text{ZnSnS}_4$ thin films and their application to solar cells, *Applied Surface Science* **334**, 180-184 (2015).
- [27] A Fairbrother, X Fontané, V Izquierdo, On the formation mechanisms of Zn-rich $\text{Cu}_2\text{ZnSnS}_4$ films prepared by sulfurization of metallic stacks. *Solar Energy Materials and Solar Cells* **112**, 97-105 (2013).
- [28] R Schurr, A Hölzing, S Jost, The crystallization of $\text{Cu}_2\text{ZnSnS}_4$ thin film solar cell absorbers from co-electroplated CuZnSn precursors. *Thin Solid Films* **517**, 2465-2468 (2009).
- [29] S.M. Pawar, A.V. Moholkar, I.K. Kim, Effect of laser incident energy on the structural, morphological and optical properties of $\text{Cu}_2\text{ZnSnS}_4$ (CZTS) thin films, *Current Applied Physics* **10**, 565-56 (2010).